

Published in final edited form as:

*Chromatographia*. 2013 January 1; 76(1-2): 13–21.

## Development of On-line Liquid Chromatography-Biochemical Detection for Soluble Epoxide Hydrolase Inhibitors in Mixtures

**David Falck,**

Department of BioMolecular Analysis, VU University Amsterdam, Amsterdam, The Netherlands

**Nils Helge Schebb,**

Department Entomology and UC Davis Comprehensive Cancer Center, University of California, Davis, CA, USA

Institute for Food Toxicology and Chemical Analysis, University of Veterinary Medicine Hannover, Hannover, Germany

**Setyo Prihatiningtyas,**

Department of BioMolecular Analysis, VU University Amsterdam, Amsterdam, The Netherlands

**Jiawen Zhang,**

Department of BioMolecular Analysis, VU University Amsterdam, Amsterdam, The Netherlands

**Ferry Heus,**

Department of BioMolecular Analysis, VU University Amsterdam, Amsterdam, The Netherlands

**Christophe Morisseau,**

Department Entomology and UC Davis Comprehensive Cancer Center, University of California, Davis, CA, USA

**Jeroen Kool,**

Department of BioMolecular Analysis, VU University Amsterdam, Amsterdam, The Netherlands

**Bruce D. Hammock, and**

Department Entomology and UC Davis Comprehensive Cancer Center, University of California, Davis, CA, USA

**Wilfried M. A. Niessen**

Department of BioMolecular Analysis, VU University Amsterdam, Amsterdam, The Netherlands  
w.m.a.niessen@vu.nl

### Abstract

In this study, an end-point-based fluorescence assay for soluble epoxide hydrolase (sEH) was transformed into an on-line continuous-flow format. The on-line biochemical detection system (BCD) was coupled on-line to liquid chromatography (LC) to allow mixture analysis. The on-line BCD was based on a flow system wherein sEH activity was detected by competition of analytes with the substrate hydrolysis. The reaction product was measured by fluorescence detection. In parallel to the BCD data, UV and MS data were obtained through post-column splitting of the LC effluent. The buffer system and reagent concentrations were optimized resulting in a stable on-line BCD with a good assay window and good sensitivity ( $S/N > 60$ ). The potency of known sEH

inhibitors (sEHs) obtained by LC–BCD correlates well with published values. The LC–BCD system was applied to test how oxidative microsomal metabolism affects the potency of three sEHs. After incubation with pig liver microsomes, several metabolites of sEHs were characterized by MS, while their individual potencies were measured by BCD. For all compounds tested, active metabolites were observed. The developed method allows for the first time the detection of sEHs in mixtures providing new opportunities in the development of drug candidates.

## Keywords

Column liquid chromatography; On-line screening; Bioassays; Enzyme inhibition; Soluble epoxide hydrolase; Metabolism

## Introduction

Soluble epoxide hydrolase (sEH) plays an important role in regulation of blood pressure, pain and inflammation [1]. In mammals, sEH is expressed in various tissues. The endogenous substrates of sEH are among others epoxyeicosatrienoic acids (EETs), which are hydrolyzed to dihydroxyeicosatrienoic acids (DHETs), thus leading to decreased blood levels of EETs. Various studies show that EETs and epoxides of other unsaturated fatty acids are anti-inflammatory, analgesic agents and lower blood pressure [2–4]. The biological levels of epoxy fatty acids can be increased by sEH inhibitors (sEHs), leading to reduction in inflammation, pain, and cardiovascular diseases in various animal models [5, 6]. Thus, sEHs are a promising new class of pharmaceutical drug candidates.

During the lead development process, metabolism studies play an important role. Not only the pharmacokinetic profile, but also the biological effects of metabolites are relevant for the action of drugs. Metabolites can be inactive, reactive, but also pharmacologically active towards the same pharmacological target or against off-targets. Screening metabolic mixtures for individual bioactive metabolites is not possible with standard end-point plate-reader-based screening methodologies. For sEH, several end-point assays have been developed, based on fluorescent detection, radiometry, and mass spectrometry [7–9]. However, these assays are only suited to screen pure compounds. The analysis of mixtures would only yield the sum of the total bioactivity of the mixture [10]. In order to assess the bioactivity of individual metabolites, fractionation has to precede the screening. As this is time-consuming, costly, and has to be performed at low resolution to prevent too much dilution, such approaches are inefficient for bioactivity profiling of metabolic mixtures [11]. One way of tackling this problem is the application of an on-line post-column screening approach, known as high-resolution screening (HRS) [12]. This technology continuously mixes bioassay reagents with the eluent after an LC separation of a mixture of compounds [13–15], such as metabolic mixtures [16]. For HRS screening with enzyme targets, like in this LC–BCD system, inhibition can be measured by detecting a decrease in the enzymatic formation of a fluorescent product. Splitting part of the LC eluent between the BCD and mass spectrometry (MS) enables correlation of bioactivity with identity for all individual metabolites [14, 17, 18].

This paper describes the development of an LC–BCD system for sEHs and its application in the efficient profiling of active oxidative metabolites. For this purpose, a fluorescence end-point plate-reader assay [7] was converted into an on-line BCD format. The on-line BCD uses the non-fluorescent substrate (3-phenyl-oxiranyl)-acetic acid cyano-(6-methoxy-naphthalen-2-yl)-methyl ester (PHOME), which is converted to the fluorescent product 6-methoxy-2-naphthaldehyde by sEH. The new analytical method was thoroughly optimized and validated. The obtained inhibition efficacy of known inhibitors compared well to

literature values. Finally, microsomal incubations of three sEHs were screened for active metabolites.

## Materials and Methods

### Materials

Human recombinant sEH was expressed and purified as described [19]. The sEH inhibitors and the substrate PHOME as well as its fluorescent product are shown in Fig. 1. Their synthesis was reported earlier: PHOME [8]; sEHi 1 [8]; sEHi 2 [20]; sEHi 3 [21]; sEHi 4 [22]; sEHi 5 [23]; sEHi 6 and sEHi 7 [24]. ELISA blocking reagent (EBR) was purchased from Roche Diagnostics (Mannheim, Germany). All other chemicals were from Sigma-Aldrich (Schnelldorf, Germany). Methanol (LC-MS Grade) and formic acid (ULC-MS Grade) were obtained from Bio-solve (Valkenswaard, The Netherlands). The water used in this study was generated with a Milli-Q academic from Millipore (Amsterdam, The Netherlands).

### Liquid Chromatography-Biochemical Detection (LC-BCD) System

The LC-BCD system shown in Fig. 2 includes separation, on-line BCD and additional parallel spectrometric detection. Separation and on-line BCD were done on an Agilent Technologies (Amstelveen, The Netherlands) 1100 LC system including a binary and two isocratic pumps, an autosampler, a column oven and a fluorescence detector. Separation was performed on a Waters (Milford, MA, USA) Atlantis dC<sub>18</sub> column (100 × 2.1 mm, 3 μm particles) at 40 °C. The mobile phase consisted of water:methanol 100:1 (v:v) as solvent A and methanol:water 100:1 (v:v) as solvent B, both containing 0.01 % formic acid. A mixture of known sEHs (125 μM each) was separated using the following gradient: 0–2 min isocratic at 50 % B, then a linear gradient to 90 % B in 43 min and isocratic at 90 % B for 4 min; afterwards a linear decrease to 50 % B in 2 min followed by 15 min re-equilibration. The LC gradient applied for the analysis of the metabolic incubations was as follows: 0–2 min isocratic at 5 % B, followed by a linear gradient to 95 % B in 43 min, isocratic at 95 % B until 49 min then a linear decrease to 5 % B in 6 min followed by 10 min re-equilibration. For analysis in flow injection analysis mode (FIA), the same set-up was used, but without the column. The LC flow-rate was 150 μL/min and the injection volume 10 μL in all cases. The flow was post-column split (see Fig. 2), directing 135 μL/min to the MS detection and 15 μL/min to the on-line BCD. In the BCD, the eluent was first mixed with 155 μL/min of a 5 nM sEH solution and incubated for 30 s. This allowed an initial interaction between analytes and enzyme. In a second step, a 30-μM solution of PHOME was added at 30 μL/min and incubated for 5 min. Here, the substrate conversion to the fluorescent product took place, which allowed detection of the enzyme activity. The incubations were done in 1.73 m straight 250 μm i.d. and 1.59 mm o.d. PTFE tubing (Sigma-Aldrich, Schnelldorf, Germany) and 2.26 m of 750 μm i.d. and 1.59 mm o.d. coiled PTFE tubing, forming 85 μL and 1 mL reactors, respectively. Both reactors were kept at 37 °C by a Grant Instruments (Shepreth, UK) water bath. The enzyme and substrate solutions were delivered by in-house built superloops which were kept on ice [25]. The fluorescence was measured at excitation of 320 ± 10 nm and emission of 460 ± 10 nm. In parallel to the on-line BCD, detection was performed by UV at 210 nm and/or by mass spectrometry.

Both techniques are able to visualize both the binders and the non-binders. In addition, MS provides structural information. The on-line BCD and the parallel UV or MS detection have different void volumes after the splitting and thus the elution times differ. The UV or MS and BCD chromatograms were aligned using a known compound, e.g., the residual parent compound in case of the metabolic incubations.

### Determination of Inhibitor Potency

The potency of five known sEHs (Fig. 1) was determined based on their apparent  $IC_{50}$  values to characterize the performance of the LC–BCD system. These sEHs have been selected in such a way that their  $IC_{50}$  values ranged from low to high nanomolar, thus covered approximately three order of magnitude of inhibitory activity. For measuring the  $IC_{50}$  values, dose–response curves were obtained by injecting the inhibitors into the LC–BCD system under isocratic conditions at 50 % methanol in FIA mode. The following concentrations and one blank were injected in duplicate per inhibitor: 0.5, 1, 2, 5, 10, 20 and 50  $\mu$ M for sEHi 1; 1, 2, 5, 10, 20, 50, 100 and 200  $\mu$ M for sEHi 2; 0.5, 1, 2, 5, 10 and 20  $\mu$ M for sEHi 3; 1, 2, 5, 10, 20, 100, 500 and 1000  $\mu$ M for sEHi 4; 0.05, 0.1, 0.2, 0.5, 1, 2 and 10  $\mu$ M for sEHi 5.

### Metabolite Identification Using Mass Spectrometry

LC–MS for metabolite identification was done either on a Bruker Daltonik (Bremen, Germany) micrOTOF-Q quadrupole time-of-flight hybrid MS, using the above described conditions, or using an ion-trap time-of-flight mass spectrometer (IT-TOF, Shimadzu, 's Hertogenbosch, The Netherlands). In the latter case, a 30-min gradient and a  $100 \times 2.1$  mm Waters XBridge  $C_{18}$  column (3.5  $\mu$ m particles) were used. Positive-ion electrospray ionization (ESI) was applied in both instrument. Other relevant instrument settings are summarized in the Supporting Information (Supplemental material 1). The mass accuracy was better than 5 ppm on both instruments. The accurate-mass data obtained were used to determine the elemental composition of the metabolites and accordingly of the fragments.

### Buffer and Compound Solutions

A 25-mM 2-bis(2-hydroxyethyl)amino-2-(hydroxymethyl)-1,3-propanediol (BIS–TRIS) buffer containing 1 g/L EBR, 1 g/L bovine serum albumin (BSA) and 0.1 g/L Tween 80 was used at pH 7.0. Stock solutions of the sEH inhibitors and PHOME were prepared at 20 mM concentrations in DMSO. sEH stocks of 100  $\mu$ M (6 mg/mL) concentration were kept at  $-80^{\circ}\text{C}$  until use and dilutions were handled on ice at all times. All PHOME and sEH dilutions were prepared in this BIS–TRIS buffer.

### Plate Reader Measurements

Plate reader-based measurements were performed to evaluate the reagent concentrations on a Victor3 plate reader from Perkin-Elmer (Groningen, The Netherlands). Black 96 'flat' bottom chimney well, polypropylene microtiter plates from Greiner bio-one (Alphen a/d Rijn, The Netherlands) were used. The total sample volume was 200  $\mu$ L and the plates were incubated at  $37^{\circ}\text{C}$ . Product formation was followed by measuring the fluorescence at  $355 \pm 4$  nm excitation and  $460 \pm 12.5$  nm emission. The PHOME concentration was 50  $\mu$ M and the sEH concentration 40 nM. Product formation was measured in 30 s intervals for 20 min under the influence of two different BSA concentrations, 0.1 g/L and 1.0 g/L. End-point measurements at 6 min were used to compare the activity of sEH under the influence of several solubilising agents. In additional experiments, the solubility of PHOME under the influence of these solubilising agents was tested in transparent plates. This was done by measuring precipitation of a 45- $\mu$ M PHOME solution by visible absorption at  $595 \pm 10$  nm.

### Microsomal Incubations

The LC–BCD/MS system was applied to investigate the metabolism of the three known sEH inhibitors sEHi 6, sEHi 1 and sEHi 7 and the bioactivity profile of their metabolites. Oxidative metabolites were generated by pig liver microsomal incubations in the presence of NADPH according to a modified version of a protocol described elsewhere [26]. In brief, reaction mixtures were prepared in 50 mM potassium phosphate buffer (pH 7.4) including 5

mM magnesium chloride. The mixtures containing 6 mM NADPH, 2.6 mg/mL pig liver microsomes and 100  $\mu$ M sEH were incubated for 2 h at 37 °C. To ensure continued availability of NADPH, 5 mM glucose-6-phosphate and 5 U/mL glucose-6-phosphate dehydrogenase were used as regenerating system. In addition, 10 % (v/v) of a 10-mM NADPH solution in the above mentioned phosphate buffer was added after 30, 60 and 90 min, respectively. The reactions were stopped by adding ice-cold acetonitrile 2:1 (v:v). The samples were then centrifuged at 16,000g for 5 min. The supernatants were taken, freeze-dried and stored at –20 °C. For the LC–BCD/MS analysis, the samples were re-dissolved in a 30 % aqueous methanol solution, providing 20-fold higher concentrations.

## Results and Discussion

### Development of an LC–BCD System for the Detection of sEH Inhibitors

The aim of this study was to develop a system for the bioactivity assessment towards sEH of individual compounds in complex mixtures. For this purpose, a homogeneous, continuous-flow detection format was applied based on the enzymatic conversion of the substrate PHOME and fluorescence readout of the reaction product (Fig. 1) [7].

Initial plate reader experiments were used as starting conditions for the optimization of the enzyme and substrate concentrations in the on-line setup. This was achieved by determining the signal-to-noise ratios (S/N) at full inhibition in the LC–BCD by injecting sEH 2 at a concentration of 100  $\mu$ M while the on-line BCD was performed at several enzyme/substrate concentration combinations. PHOME was applied at concentrations of 4.5, 2.3 and 1.2  $\mu$ M in combination with a sEH concentration of 4 nM. Concentrations of 40, 8 and 4 nM sEH were tested at a PHOME concentration of 4.5  $\mu$ M. Finally, a mixture of 4 nM sEH and 4.5  $\mu$ M PHOME was incubated off-line for 30, 45, 60 or 90 min and directly infused into the fluorescence detector to assess the fluorescence intensity at full substrate conversion.

In contrast to the earlier developed end-point plate-reader assay, an on-line format requires a shorter incubation time. The BCD system was set up with a 5 min reaction time to minimize band broadening in the LC–BCD system. In order to increase the solubility of PHOME at room temperature, 0.1 g/L Tween 80 were added to the buffer without measurable influence on the enzymatic conversion (data not shown). The substrate was used close to its limit of solubility (30  $\mu$ M) in the superloop, thus with a substrate concentration of 4.5  $\mu$ M in the reaction coil (Fig. 2). This concentration is lower than the Michaelis–Menten-constant ( $K_M$ ) of PHOME for sEH, which is above its limit of solubility [8]. Thus, at a concentration of 4.5  $\mu$ M of PHOME, the enzyme is not in saturating condition allowing the sensitive detection of inhibitors. Additional actions to shorten the reaction time comprise a BSA concentration of 1.0 g/L rather than 0.1 g/L.

The enzyme concentration was adjusted to yield about 20 % substrate conversion in a 5-min reaction time. This low percentage of conversion ensures that the reaction is still in the initial conversion stage where no significant rate and concentration limiting effects are observed. It was found that only 4 nM sEH in the reaction coil were sufficient, which is almost identical to the concentration of 3 nM in the end-point method [7].

Figure 3 shows the most important BCD parameters and demonstrates that the reaction causing the BCD baseline is of enzymatic nature. Section 1 of Fig. 3 shows the background level of fluorescence generated with buffer-filled superloops. When the PHOME substrate solution was introduced (point 2 in Fig. 3), the fluorescence signal somewhat increased due to fluorescence of the substrate and/or autohydrolysis and/or presence of trace amount of the fluorescent product in the substrate (section 3 in Fig. 3). After the enzyme is added to the other superloop (point 4 in Fig. 3), a rapid increase in the signal is observed resulting in a

stable baseline due to the steady state of the enzymatic reaction (section 5 in Fig. 3). When cooling the reaction coil on ice (point 7 in Fig 3), the signal returns to the baseline of the substrate solution (section 8 in Fig 3). The absence of conversion under these conditions clearly demonstrates that the increased fluorescence signal is caused by the enzymatic conversion of PHOME to its fluorescent product.

The most important parameter of the BCD system is the difference between the steady state of the reaction serving as baseline of BCD and the background signal (number 6 in Fig. 3, indicating the difference in fluorescence signal between section 5 and section 8 in Fig. 3), also known as assay window. In this case, the assay window is nine times higher than the substrate fluorescence. Together with the stability of the signal, a S/N ratio of 70 results between full inhibition of sEH and the steady state, allowing a detection of as little as 5 % inhibition of the added sEH. In conclusion, the data quality of the on-line BCD is more than adequate to detect the significant part of the sigmoidal dose–response behavior of inhibitors between 10 and 90 % inhibition.

As the sEHs are introduced into the on-line BCD from an LC setup, their activity is visualized as a negative chromatographic peak, which is a result of the indirect enzymatic activity measurement: higher inhibitor activity means less fluorescent product formation. Furthermore, the dose–response behavior in the on-line BCD changes to a sigmoidal one due to the underlying competitive biophysical interactions between enzyme, substrate and inhibitor. All this is apparent from Fig. 4a where the overlaid BCD chromatograms of a dilution series of several sEH 1 concentrations are shown.

### Characterization of the LC–BCD System

The performance of the LC–BCD system to quantitatively measure the potency of sEHs was tested by analysis of five known inhibitors at different concentrations in FIA mode, which is a fast way to measure  $IC_{50}$  values if pure compounds are available. As shown in Fig. 4a, the injection of sEH 1 resulted in negative peaks in the BCD chromatogram with increasing negative peak heights upon injecting increasing concentrations. The variance in peak height between duplicate injections was generally lower than 10 % (in 90 % of 36 samples). As previously shown for various enzymes, the negative peak height in LC–BCD systems can be used to calculate the percentage of inhibition [18, 27]. Based on the resulting dose–response curves (Fig. 4b), it is possible to quantitatively rank the sEHs by their potency. Among the compounds tested, sEH 5 was the most active and sEH 4 the least active inhibitor. In order to deduce  $IC_{50}$  values for each compound, the dilution of the injected amount of inhibitor in the LC–BCD system has to be taken into account [18, 28]. The dilution results from the mixing of LC eluent and BCD reagents ( $D_m$ ), which depends on the flow rates of eluent entering the on-line BCD ( $u_E$ ) and the total flow at detection ( $u_F$ ).

$$D_m = \frac{u_F}{u_E} \quad (1)$$

In addition, inhibitors injected are also diluted due to their residence time in the flow system ( $D_C$ ). In a test tube or well plate experiment, the inhibitor can be assumed to be evenly distributed after mixing. The same is only true for the diagonal distribution in the on-line BCDs. In the longitudinal dimension, which is reflected on the time axis, the inhibitor is distributed according to a near-Gaussian distribution which is typical to chromatography. This phenomenon is a result of longitudinal diffusion of the initially homogeneous injection plug ( $V_i$ ). It further dilutes the injected concentration ( $c_i$ ). The full width at half maximum (FWHM) and the flow rate ( $u_C$ ) have to be derived from the same chromatogram, preferably from the BCD chromatogram which results in  $u_C = u_F$ .



$$D_c = \frac{\text{FWHM}}{2} \times \sqrt{\frac{\pi}{\ln 2}} \times \frac{u_c}{V_i} \quad (2)$$

Therefore, the final concentration at the maximum negative peak height ( $c_F$ ), which can be calculated from Eq. 3, was used for the dose–response curves.

$$c_F = \frac{c_i}{D_M \times D_C} \quad (3)$$

Thus, the dilution factors are calculated individually for every measurement, and they range from 71 to 210. The final concentrations were plotted against the corresponding percentages of inhibition and the data fitted with GraphPadPrism (GraphPad Software, La Jolla, USA). This results in the sigmoidal dose–response curves shown in Fig. 4b. The reproducibility of the data points measured (see above) and the quality of all the fits, expressed by resulting  $R^2$ -values of  $>0.975$ , are further indications of the high data quality.

The calculated  $IC_{50}$  values for the five compounds tested are given in Table 1. They covered a range of about three orders of magnitude. This demonstrates that the developed LC–BCD method allows the measurement/detection of highly potent as well as weak sEHs. The potency of sEHi 5 was remarkably high, with an apparent  $IC_{50}$  value of 2 nM. Given an enzyme concentration of 4 nM in the reaction coil, this is the highest potency which can be observed with the setup [9]. Most importantly, the newly developed LC–BCD method ranked the potency of the tested inhibitors in the same order as commonly employed end-point assays, except for sEHi 2 (Table 1). However, for few sEHs, the determined  $IC_{50}$  differed significantly from literature values: For sEHi 2, the observed potency by LC–BCD was about 20-fold higher compared to the value from an end-point assay, while the measured  $IC_{50}$  value for sEHi 4 was about 4-fold higher than previously reported (Table 1). Similar to our observations, up to 20-fold differences have been described between different sEH assays, because the measured potency for individual sEHs is substrate-dependent [9]. This observation is substantiated with the results for sEHi 1. For this compound, using the same substrate, a very good agreement was found between our data and the literature [7]. The potencies for sEHi 3 and sEHi 5 are also consistent with literature values, despite use of different substrates (Table 1). Overall, the results from the analysis of individual sEHs in the LC–BCD system show that the negative peak height is a suitable quantitative measure for the potency of inhibitors, and that the data obtained are in good agreement with other methods to characterize the potency of sEHs.

In contrast to end-point assays, the LC–BCD system combines identity and activity detection after chromatographic separation. It thus allows assessment of individual compounds in mixtures. This is demonstrated by analysing a mixture of sEHi 6, sEHi 1, sEHi 7, and two compounds without sEH activity, diclofenac and phenylbutazone. In this case, the BCD signal shows only three major peaks, which corresponded well with the elution times to the three sEHs, whereas in the corresponding LC–UV or LC–MS all five compounds are observed (data not shown). These experiments show that the developed LC–BCD system allows assessing the bioactivity of individual compounds in mixtures. In only one analysis step, it can distinguish between active and non-active compounds in mixtures.

### Application of LC–BCD on the Analysis of Metabolic Mixtures of sEHs

In order to demonstrate the applicability of the LC–BCD system to the analysis of unknown mixtures, in vitro microsomal incubations of three sEHs were analysed. The LC–MS data

showed that each compound was metabolized to several metabolites (Fig. 5). By combining BCD traces and MS extracted ion chromatograms, the peaks of active compounds can be directly identified and structurally characterized.

For sEHi 6, three bioactivity peaks were observed (Fig. 5a). The main peak eluting around 43.2 min in LC–MS, peak A4<sup>MS</sup>, corresponding to peak AIII<sup>BCD</sup> in LC–BCD, is the parent compound (protonated molecule  $[M + H]^+$  with  $m/z$  277.228). The three peaks A1<sup>MS</sup>, A2<sup>MS</sup> and A3<sup>MS</sup>, eluting at 35.0, 35.8 and 38.0 min, respectively, in LC–MS, were not observed in the control incubations (data not shown). These compounds could be tentatively identified as hydroxylated metabolites because all contained an additional oxygen compared to the parent compound ( $[M + H]^+$  with  $m/z$  293.223). While peak A1<sup>MS</sup> is not bioactive, peaks A2<sup>MS</sup> and A3<sup>MS</sup> correspond to the peaks AI<sup>BCD</sup> and AII<sup>BCD</sup>, respectively. Note that peak A3<sup>MS</sup> consists of three non-separated compounds thus three different mono-hydroxylated metabolites with  $m/z$  293.209, which were not well separated. The peaks A5<sup>MS</sup> and A6<sup>MS</sup> are present as contaminants; they show the same nominal mass as the oxygenated metabolites and the parent sEHi 6, but different accurate mass ( $m/z$  293.209 and 277.217, respectively).

The LC–BCD chromatogram of the metabolic incubation trace of sEHi 1 showed four peaks (Fig. 5b). The main peak BIV<sup>BCD</sup> corresponds to peak B9<sup>MS</sup>, the parent compound ( $[M + H]^+$  with  $m/z$  227.214). In this case, six mono-hydroxylated metabolites (B2<sup>MS</sup> through B7<sup>MS</sup>,  $[M + H]^+$  with  $m/z$  243.208) were observed (Fig. 5b). These metabolites gave rise to peaks BI<sup>BCD</sup> and BII<sup>BCD</sup>. By careful evaluation of the peak shapes and retention times, it may be concluded that B2<sup>MS</sup> and at least two of the metabolites B4<sup>MS</sup> to B7<sup>MS</sup> are bioactive. The oxidated dehydrogenated metabolite B1<sup>MS</sup> ( $[M + H]^+$  with  $m/z$  241.192) is clearly not bioactive, whereas the peak shape of the dehydrogenated metabolite B8<sup>MS</sup> ( $[M + H]^+$  with  $m/z$  225.197) matched the retention time of BIII<sup>BCD</sup>. This is an excellent example of the added value of the LC–BCD approach: whereas the minor peak B8<sup>MS</sup> would be easily ignored in an MS-only approach, its strong corresponding peak BIII<sup>BCD</sup> cannot be overlooked.

Compared to sEHi 6 and sEHi 1, sEHi 7 showed less metabolic conversion: only two mono-hydroxylated metabolites were detected ( $[M + H]^+$  with  $m/z$  409.306) (Fig. 5c). The main peaks CII<sup>BCD</sup> and C3<sup>MS</sup> correspond to the parent compound ( $[M + H]^+$  with  $m/z$  393.312). The two metabolites C1<sup>MS</sup> and C2<sup>MS</sup> are not well separated and result in only one peak in the LC–BCD chromatogram. The retention time of C1<sup>MS</sup> corresponds to the peak CI<sup>BCD</sup>, indicating the compound is bioactive, but the increased tailing of CI<sup>BIO</sup> suggests that C2 is bioactive as well.

All three sEHIs were metabolized in the aliphatic chains and rings at either side of the urea function. A more detailed structural analysis was not possible as MS fragmentation only occurred in or next to the urea function. For all three sEHIs tested, LC–BCD/MS analysis allowed the tentative identification of at least two inhibitory active metabolites. In only a single step analysis of 60 min, active metabolites can be detected. Moreover, it is possible to distinguish between active and non-active metabolites and to characterize bioactive compounds by their inhibitory potency and MS spectra.

## Conclusion

A new LC–BCD system for the detection of sEHIs in complex mixtures has been developed. The detection principle is a continuous-flow enzyme activity assay coupled on-line to LC with parallel MS detection. The substrate PHOME allowed sensitive and robust monitoring of bioactivity by fluorescence. After thorough optimization of the assay conditions, the



incubation time in the BCD was reduced from 60 to 5.5 min. With a sEH concentration of only 4 nM in the reaction coil, the S/N ratio for complete sEH inhibition was still higher than 60. Analysis of several known sEHs demonstrated that the peak height, observed in LC–BCD can be used as quantitative measure for sEH inhibition. Moreover, the obtained potencies, measured as IC<sub>50</sub> values, for sEHs are in good agreement with previously reported values. The LC–BCD system is able to perform bioactivity analysis of individual compounds in mixtures. This was successfully demonstrated by the analysis of a standard mixture as well as of in vitro metabolic conversions of three known sEHs containing both active and non-active metabolites towards sEH. Here, LC–BCD revealed the formation of new active metabolites, which could be simultaneously characterized by LC–MS.

With the developed LC–BCD system, inhibitors can be detected and characterized in a single analysis. Given the increasing interest in sEH as drug-target for various diseases, this new technique may pave the route for the detection of new classes of sEHs in natural products or crude mixtures arising from organic synthesis. Moreover, metabolism studies with LC–BCD as read out will allow the identification of active metabolites in early stages of lead development and thus assist the identification of the best compounds as drug candidates.

## Acknowledgments

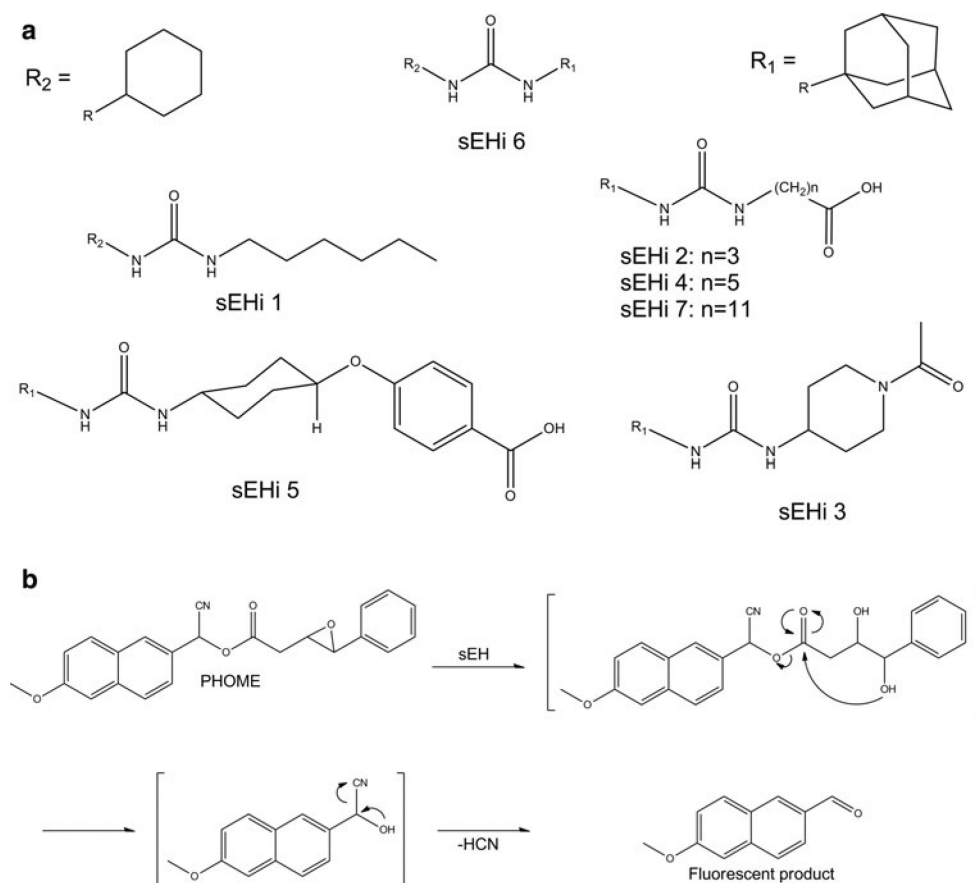
This study was supported by NIEHS (R01 ES002710, P42 ES004699), NIOSH (PHS OH07550) and the German Academic Exchange Service. B.D.H is as senior fellow of the American Asthma Society. We acknowledge Lionel Blanchet for his help with data management.

## References

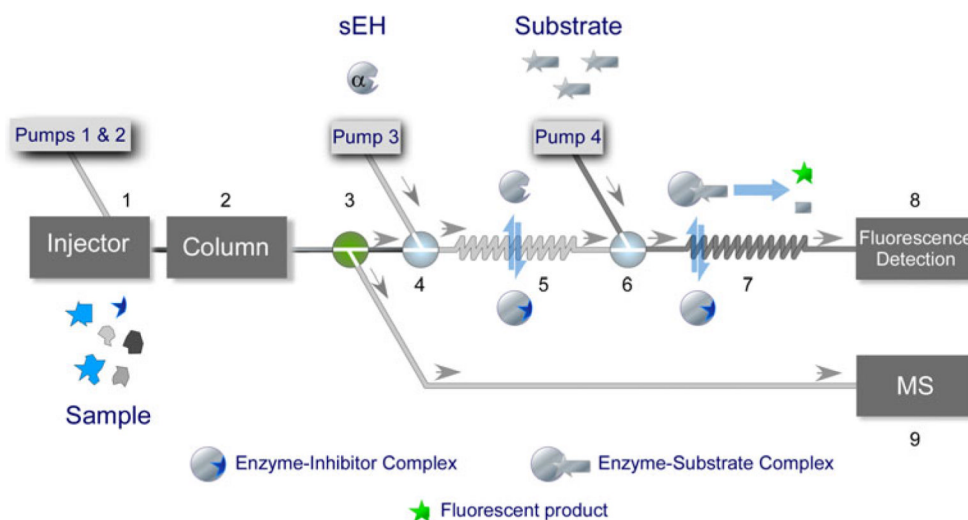
1. Newman JW, Morisseau C, Hammock BD. Epoxide hydrolases: their roles and interactions with lipid metabolism. *Prog Lipid Res.* 2005; 44:1–51. [PubMed: 15748653]
2. Certikova Chabova V, Walkowska A, Kompanowska-Jezierska E, Sadowski J, Kujal P, Vernerova Z, Vanourkova Z, Kopkan L, Kramer HJ, Falck JR, Imig JD, Hammock BD, Vaneckova I, Cervenka L. Combined inhibition of 20-hydroxyeicosatetraenoic acid formation and of epoxyeicosatrienoic acids degradation attenuates hypertension and hypertension-induced end-organ damage in Ren-2 transgenic rats. *Clin Sci (Lond).* 2011; 118:617–632. [PubMed: 20050826]
3. Schmelzer KR, Kubala L, Newman JW, Kim IH, Eiserich JP, Hammock BD. Soluble epoxide hydrolase is a therapeutic target for acute inflammation. *Proc Natl Acad Sci USA.* 2005; 102:9772–9777. [PubMed: 15994227]
4. Inceoglu B, Wagner K, Schebb NH, Morisseau C, Jinks SL, Ulu A, Hegedus C, Rose T, Brosnan R, Hammock BD. Anal-gesia mediated by soluble epoxide hydrolase inhibitors is dependent on cAMP. *Proc Natl Acad Sci USA.* 2011; 108:5093–5097. [PubMed: 21383170]
5. Imig JD, Zhao X, Zaharis CZ, Olearczyk JJ, Pollock DM, Newman JW, Kim IH, Watanabe T, Hammock BD. An orally active epoxide hydrolase inhibitor lowers blood pressure and provides renal protection in salt-sensitive hypertension. *Hypertension.* 2005; 46:975–981. [PubMed: 16157792]
6. Imig JD, Hammock BD. Soluble epoxide hydrolase as a therapeutic target for cardiovascular diseases. *Nat Rev Drug Discovery.* 2009; 8:794–805.
7. Wolf NM, Morisseau C, Jones PD, Hock B, Hammock BD. Development of a high-throughput screen for soluble epoxide hydrolase inhibition. *Anal Biochem.* 2006; 355:71–80. [PubMed: 16729954]
8. Jones PD, Wolf NM, Morisseau C, Whetstone P, Hock B, Hammock BD. Fluorescent substrates for soluble epoxide hydrolase and application to inhibition studies. *Anal Biochem.* 2005; 343:66–75. [PubMed: 15963942]

9. Schebb NH, Huby M, Morisseau C, Hwang SH, Hammock BD. Development of an online SPE-LC-MS-based assay using endogenous substrate for investigation of soluble epoxide hydrolase (sEH) inhibitors. *Anal Bioanal Chem.* 2011; 400:1359–1366. [PubMed: 21479549]
10. Ulu A, Davis BB, Tsai HJ, Kim IH, Morisseau C, Inceoglu B, Fiehn O, Hammock BD, Weiss RH. Soluble epoxide hydrolase inhibitors reduce the development of atherosclerosis in apolipoprotein e-knockout mouse model. *J Cardiovasc Pharmacol.* 2008; 52:314–323. [PubMed: 18791465]
11. Ebada SS, Edrada RA, Lin W, Proksch P. Methods for isolation, purification and structural elucidation of bioactive secondary metabolites from marine invertebrates. *Nat Protoc.* 2008; 3:1820–1831. [PubMed: 18989260]
12. Kool J, Giera M, Irth H, Niessen WMA. Advances in mass spectrometry-based post-column bioaffinity profiling of mixtures. *Anal Bioanal Chem.* 2011; 399:2655–2668. [PubMed: 21107824]
13. Schebb NH, Faber H, Maul R, Heus F, Kool J, Irth H, Karst U. Analysis of glutathione adducts of patulin by means of liquid chromatography (HPLC) with biochemical detection (BCD) and electrospray ionization tandem mass spectrometry (ESI-MS/MS). *Anal Bioanal Chem.* 2009; 394:1361–1373. [PubMed: 19390846]
14. Marques LA, Kool J, de Kanter FJJ, Lingeman H, Niessen WMA, Irth H. Production and on-line acetylcholinesterase bio-activity profiling of chemical and biological degradation products of tacrine. *J Pharm Biomed Anal.* 2010; 53:609–616. [PubMed: 20466502]
15. Kool J, van Liempd SM, Harmsen S, Beckman J, van Elswijk D, Commandeur JNM, Irth H, Vermeulen NPE. Cytochrome P450 bio-affinity detection coupled to gradient HPLC: on-line screening of affinities to cytochrome P4501A2 and 2D6. *J Chromatogr B.* 2007; 858:49–58.
16. Van Liempd SM, Kool J, Meerman JH, Irth H, Vermeulen NPE. Metabolic profiling of endocrine-disrupting compounds by on-line cytochrome p450 bioreaction coupled to on-line receptor affinity screening. *Chem Res Toxicol.* 2007; 20:1825–1832. [PubMed: 17975887]
17. de Vlieger JSB, Kolkman AJ, Ampt KA, Commandeur JNM, Vermeulen NPE, Kool J, Wijmenga SS, Niessen WMA, Irth H, Honing M. Determination and identification of estrogenic compounds generated with biosynthetic enzymes using hyphenated screening assays, high resolution mass spectrometry and off-line NMR. *J Chromatogr B.* 2010; 878:667–674.
18. Falck D, de Vlieger JSB, Niessen WMA, Kool J, Honing M, Giera M, Irth H. Development of an online p38alpha mitogen-activated protein kinase binding assay and integration of LC-HR-MS. *Anal Bioanal Chem.* 2010; 398:1771–1780. [PubMed: 20730527]
19. Beetham JK, Tian T, Hammock BD. cDNA cloning and expression of a soluble epoxide hydrolase from human liver. *Arch Biochem Biophys.* 1993; 305:197–201. [PubMed: 8342951]
20. Kim IH, Morisseau C, Watanabe T, Hammock BD. Design, synthesis, and biological activity of 1,3-disubstituted ureas as potent inhibitors of the soluble epoxide hydrolase of increased water solubility. *J Med Chem.* 2004; 47:2110–2122. [PubMed: 15056008]
21. Jones PD, Tsai HJ, Do ZN, Morisseau C, Hammock BD. Synthesis and SAR of conformationally restricted inhibitors of soluble epoxide hydrolase. *Bioorg Med Chem Lett.* 2006; 16:5212–5216. [PubMed: 16870439]
22. Olearczyk JJ, Field MB, Kim IH, Morisseau C, Hammock BD, Imig JD. Substituted adamantyl-urea inhibitors of the soluble epoxide hydrolase dilate mesenteric resistance vessels. *J Pharmacol Exp Ther.* 2006; 318:1307–1314. [PubMed: 16772540]
23. Hwang SH, Tsai HJ, Liu JY, Morisseau C, Hammock BD. Orally bioavailable potent soluble epoxide hydrolase inhibitors. *J Med Chem.* 2007; 50:3825–3840. [PubMed: 17616115]
24. Morisseau C, Goodrow MH, Newman JW, Wheelock CE, Dowdy DL, Hammock BD. Structural refinement of inhibitors of urea-based soluble epoxide hydrolases. *Biochem Pharmacol.* 2002; 63:1599–1608. [PubMed: 12007563]
25. Falck D, de Vlieger JSB, Giera M, Honing M, Irth H, Niessen WMA, Kool J. On-line electrochemistry-bioaffinity screening with parallel HR-LC-MS for the generation and characterization of modified p38alpha kinase inhibitors. *Anal Bioanal Chem.* 2012; 403:367–375. [PubMed: 22227812]
26. Kool J, Ramautar R, van Liempd SM, Beckman J, de Kanter FJJ, Meerman JH, Schenk T, Irth H, Commandeur JNM, Vermeulen NPE. Rapid on-line profiling of estrogen receptor binding metabolites of tamoxifen. *J Med Chem.* 2006; 49:3287–3292. [PubMed: 16722647]

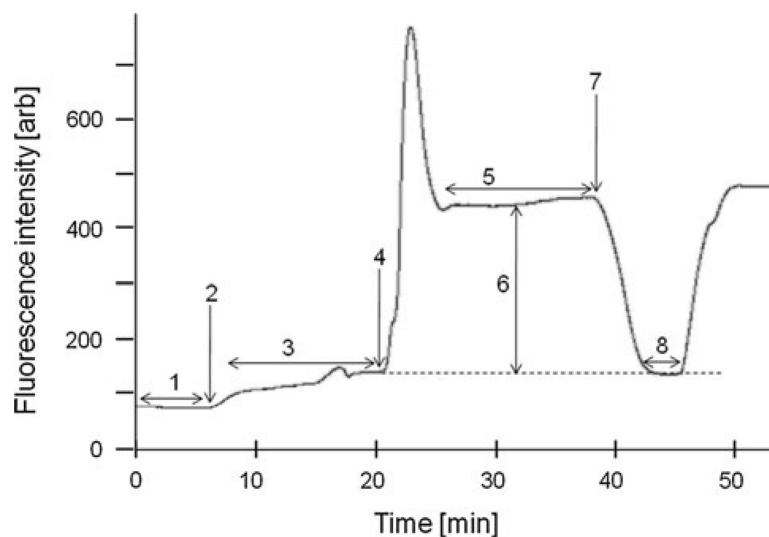
27. Kool J, Eggink M, van Rossum H, van Liempd SM, van Elswijk DA, Irth H, Commandeur JNM, Meerman JH, Vermeulen NPE. Online biochemical detection of glutathione-S-transferase P1-specific inhibitors in complex mixtures. *J Biomol Screen*. 2007; 12:396–405. [PubMed: 17379858]
28. Schebb NH, Heus F, Saenger T, Karst U, Irth H, Kool J. Development of a countergradient parking system for gradient liquid chromatography with online biochemical detection of serine protease inhibitors. *Anal Chem*. 2008; 80:6764–6772. [PubMed: 18686973]



**Fig. 1.** Structures of **a** the sEHs used in this study, and **b** the reaction scheme of the substrate PHOME to its fluorescent product

**Fig. 2.**

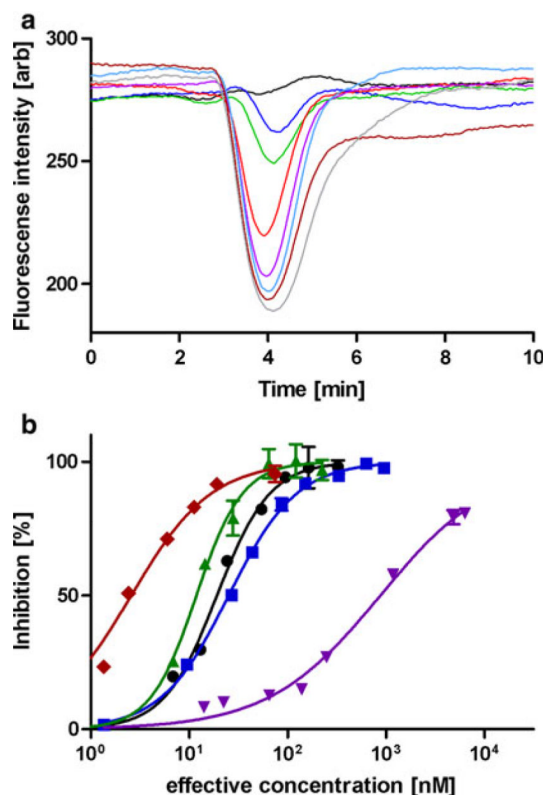
Setup of the LC-BCD system. The system combines separation, on-line BCD and additional UV or MS detection in parallel. It includes 1 autoinjector, 2 reversed-phase LC column, 3 flow-splitting between parallel 9 UV or ESI-MS detection and 4–8 the on-line BCD. The BCD comprises of 4 mixing of LC effluent and an sEH solution, 5 incubation with the enzyme, followed by 6 mixing of PHOME solution, 7 incubation with PHOME, and finally 8 fluorescence detection



**Fig. 3.**

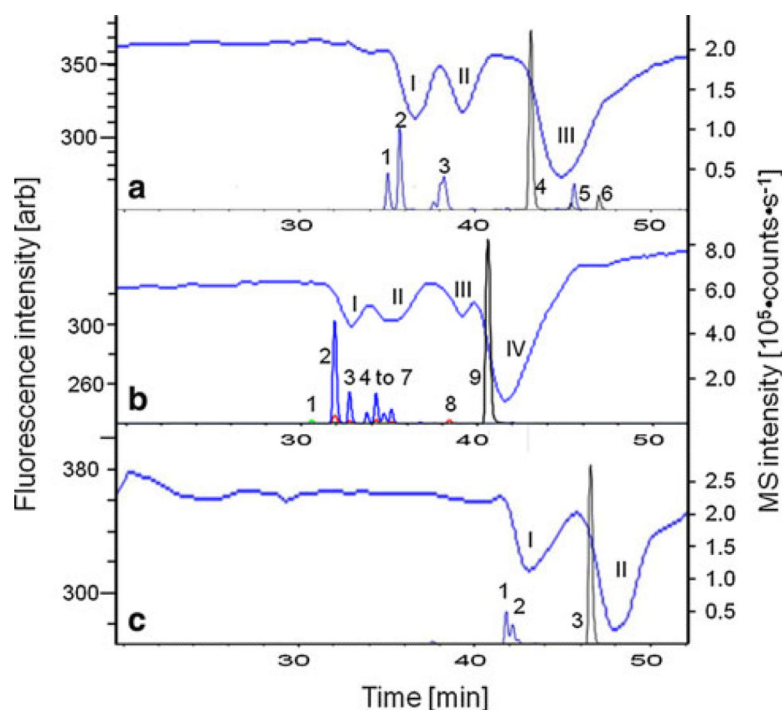
Analysis of BCD parameters. Several sections of the graph are highlighted by *horizontal double-headed arrows* in contrast to important time points which are highlighted by *vertical arrows*. Sections 1, 3 and 8 show the buffer, the substrate related and the complete background levels of fluorescence, respectively. Furthermore, section 5 depicts the baseline due to the enzymatic reaction. The points 2 and 4 mark the introduction of the PHOME substrate solution and of the sEH enzyme solution, respectively. Point 7 indicates the start of the cooling of the incubation tubing, which stops the enzymatic conversion in section 8. The difference between the fluorescence at full steady state reaction (section 5) and the combined fluorescence background at completely stopped reaction (section 8), as indicated by a *vertical double-headed arrow* (number 6), indicates the assay window. The eight numbers are explained in more detail in the text





**Fig. 4.**

Analysis of sEH in FIA mode. **a** BCD signals of injections (10 µL) of eight different concentrations of sEH 1 [blank (*black*), 0.5 µM (*blue*), 1 µM (*green*), 2 µM (*red*), 5 µM (*violet*), 10 µM (*light blue*), 20 µM (*brown*) and 50 µM (*grey*)]. The percentage of sEH inhibition, calculated from the negative peak height, is plotted against the inhibitor concentration for five different sEHs in panel **b** [sEH 1 (*black circles*), sEH 2 (*blue squares*), sEH 3 (*green triangles*), sEH 4 (*purple inverted triangles*) and sEH 5 (*red diamonds*)]. Mean and range of a determination in duplicate are shown. The concentration is given as final concentration of the inhibitor in the reaction coil, taking a dilution factor into account

**Fig. 5.**

Analysis of oxidative microsomal incubations of three sEH inhibitors by the LC-BCD/MS system. In *each panel*, the LC-BCD chromatogram (*blue line*) is combined with the MS trace (*black, red, green*). **a** sEHi 6, **b** sEHi 1, and **c** sEHi 7. The *peaks* are labelled in order of retention time with Arabic (MS) or Latin (BCD) numbers

**Table 1**IC<sub>50</sub> values determined for sEHi 1–5 and comparison to literature values

| Compound | LC–BCD system (nM) <sup>a</sup> | Literature values (nM) | Substrate          |
|----------|---------------------------------|------------------------|--------------------|
| sEHi 1   | 19 (1)                          | 29 ± 13 [7]            | PHOME              |
| sEHi 2   | 25 (1)                          | 684 [22]               | CMNPC <sup>b</sup> |
| sEHi 3   | 12 (2)                          | 15 [23]                | CMNPC <sup>b</sup> |
| sEHi 4   | 880 (90)                        | 171 [22]               | CMNPC <sup>b</sup> |
| sEHi 5   | 2.6 (0.6)                       | 2 [23]                 | CMNPC <sup>b</sup> |

<sup>a</sup>Mean and difference (in brackets) from individual fitting of the duplicate curves<sup>b</sup>Cyano(2-methoxynaphthalen-6-yl)methyl *trans*-(3-phenyloxyran-2-yl)methylcarbonate